

¹ The Morphological Diversification of Siphonophore Tentilla

³ Alejandro Damian-Serrano^{1,‡}, Steven H.D. Haddock², Casey W. Dunn¹

⁴ ¹ Yale University, Department of Ecology and Evolutionary Biology, 165 Prospect St.,
⁵ New Haven, CT 06520, USA

⁶ ² Monterey Bay Aquarium Research Institute, 7700 Sandholdt Rd., Moss Landing, CA
⁷ 95039, USA

⁸ [‡] Corresponding author: Alejandro Damian-Serrano, email: alejandro.damianserrano@
⁹ yale.edu

¹⁰ Abstract

¹¹ Siphonophores are free-living predatory colonial hydrozoan cnidarians found in every ocean
¹² of the world. Siphonophore tentilla (tentacle side branches) are unique biological structures
¹³ for prey capture, composed of a complex arrangement of cnidocytes (stinging cells) bearing
¹⁴ different types of nematocysts (stinging capsules) and auxiliary structures. Tentilla present
¹⁵ an extensive morphological and functional diversity across species. While associations
¹⁶ between tentilla form and diet have been reported, the evolutionary history giving rise
¹⁷ to this morphological diversity is largely unexplored. Here we examine the evolutionary
¹⁸ gains and losses of novel tentillum substructures and nematocyst types on the most recent
¹⁹ siphonophore phylogeny. Tentilla have a precisely coordinated high-speed strike mechanism
²⁰ of synchronous unwinding and nematocysts discharge. Here we characterize the kinematic
²¹ diversity of this prey capture reaction using high-speed video and find relationships with
²² morphological characters. Since tentillum discharge occurs in synchrony across a broad
²³ morphological diversity, we evaluate how phenotypic integration is maintaining character
²⁴ correlations across evolutionary time. We found that the the tentillum morphospace has
²⁵ low dimensionality, we identified instances of heterochrony and morphological convergence,

26 and generated hypotheses on the diets of understudied siphonophore species. Our findings
27 indicate that siphonophore tentilla are phenotypically integrated structures with a complex
28 evolutionary history leading to a phylogenetically structured diversity of forms which are
29 predictive of kinematic performance and feeding habits.

30 **Keywords**

31 Siphonophore, tentilla, nematocysts, character evolution

32 **Introduction**

33 Siphonophores have fascinated zoologists for centuries for their extremely subspecialized
34 colonial organization and integration. Today we have a comprehensive taxonomic coverage
35 on the morphological diversity of this group due to the extensive work of siphonophore
36 taxonomists in the past few decades (1–10), which has been elegantly synthesized in detailed
37 synopsis (11). In addition, recent advances in phylogenetic analyses of siphonophores (13, 14)
38 have provided a macroevolutionary context to interpret this diversity. With these assets in
39 hand, we can now begin to study siphonophores from an orthogonal perspective, focusing on
40 the diversity and evolutionary history of specific structures. Here we focus on one of such
41 structures: the tentilla. Like many cnidarians, siphonophore tentacles bear side branches
42 (tentilla) with nematocysts (Fig. 1). But unlike other cnidarians, most siphonophore tentilla
43 are dynamic structures that react to prey encounters by rapidly unfolding the nematocyst
44 battery to slap around the prey. This maximizes the surface area of contact between the
45 nematocysts and the prey they fire upon. In addition, siphonophore tentilla present a
46 remarkable diversity of morphologies (Fig. 2), sizes, and nematocyst complements (Fig. 3).
47 Our overarching aim is to organize all this phenotypic diversity in a phylogenetic context,
48 and identify the evolutionary processes that generated it.

49 In (14), we collected the most extensive morphological dataset on siphonophore tentilla and
50 nematocysts using state-of-the-art microscopy techniques, and expanded the taxon sampling

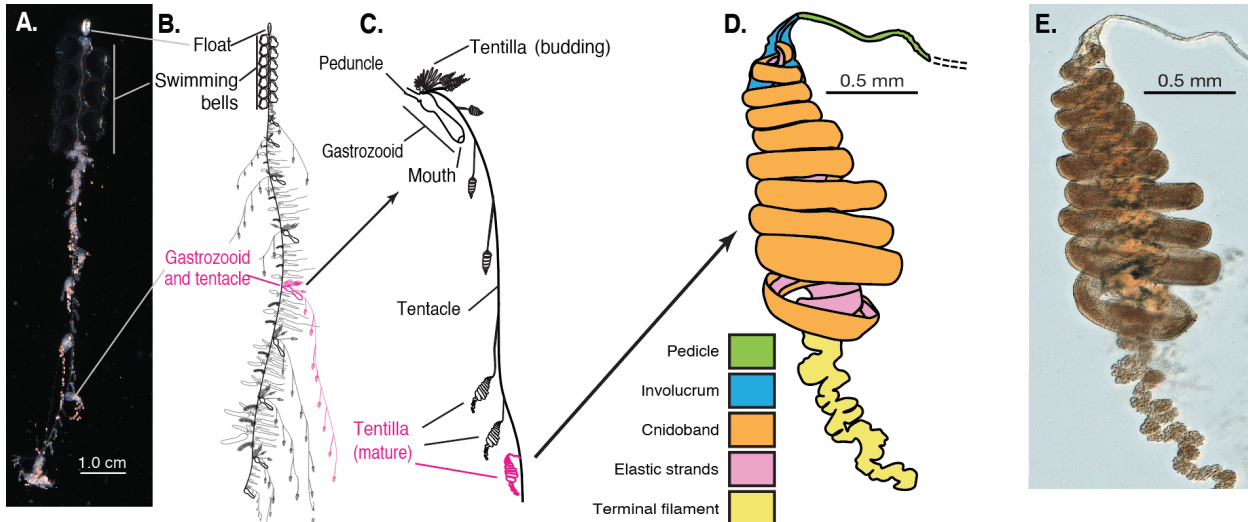


Figure 1: Siphonophore anatomy. A - *Nanomia* sp. siphonophore colony (photo by Catriona Munro). B, C - Illustration of a *Nanomia* colony, gastrozooid, and tentacle closeup (by Freya Goetz). D - *Nanomia* sp. Tentillum illustration and main parts. E - Differential interference contrast micrograph of the tentillum illustrated in D. Figure reproduced from Damian-Serrano et al. 2020 with permission.

51 of the phylogeny to disentangle the evolutionary history. The analyses we carried out led
 52 to novel, generalizable insights into the evolution of predatory specialization. The primary
 53 findings of that work were that generalists evolved from crustacean-specialist ancestors, and
 54 that feeding specializations were associated with distinct modes of evolution and character
 55 integration patterns. The work we present here is complementary to (14), showcasing a far
 56 more detailed account on the evolutionary history of tentilla morphology.

57 Nematocysts are unique biological weapons for defense and prey capture exclusive to
 58 the phylum Cnidaria. Mariscal ((15)) reported that hydrozoans have the largest diversity
 59 of nematocyst types among cnidarians. Among them, siphonophores present the greatest
 60 variety of types (12), and vary widely across taxa in which and how many types they carry
 61 on their tentacles (Fig. 3). Werner (16) noted that there are nine types of nematocyst
 62 found in siphonophores, of which four, anacrophore rhopalonemes, acrophore rhopalonemes,
 63 homotrichous anisorhizas, and birhopaloids, are unique to them. Heteroneme and haploneme
 64 nematocysts serve penetrant and entangling functions, while rhopalonemes and desmonemes

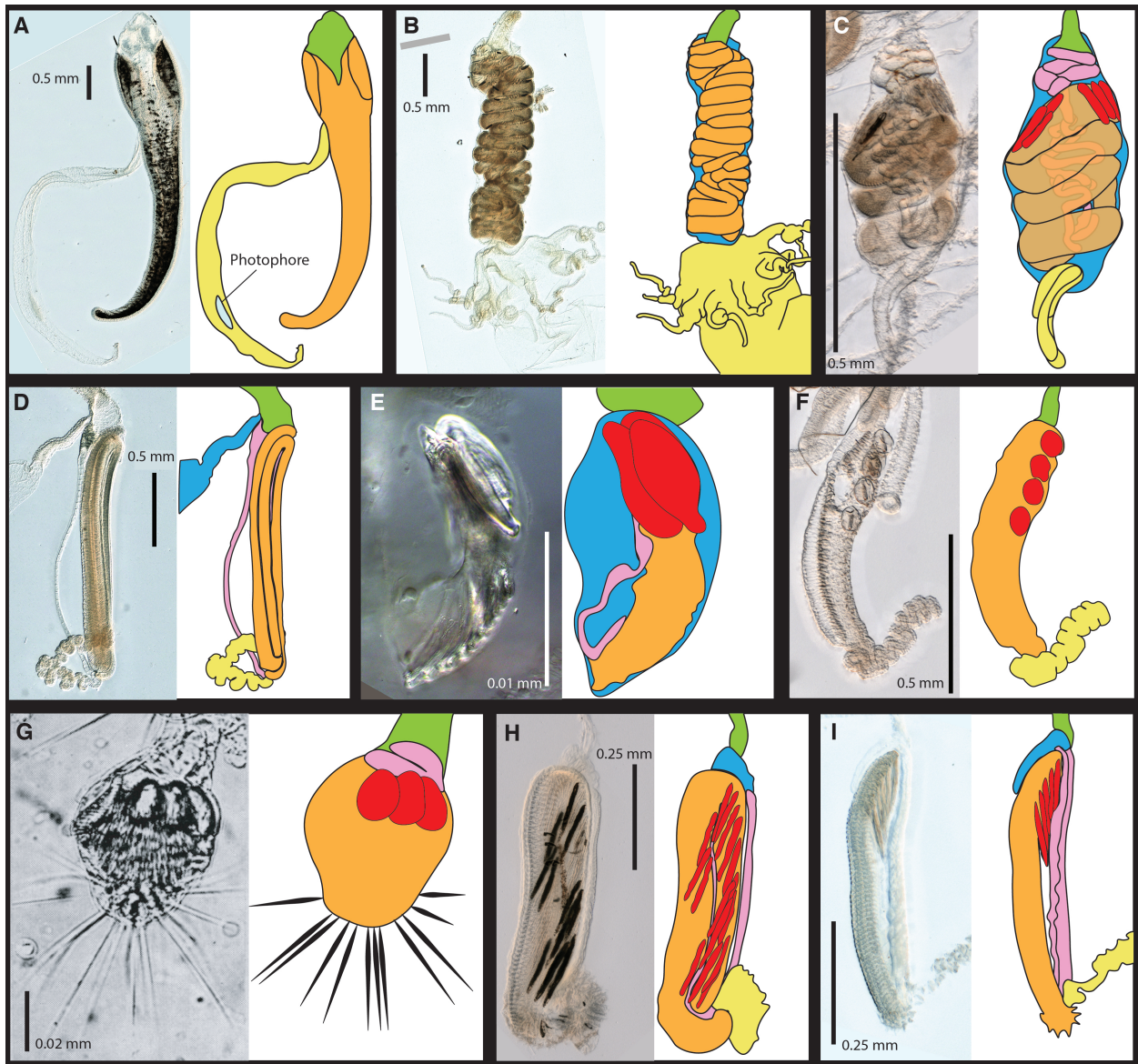


Figure 2: Tentillum diversity. The illustrations delineate the pedicle (green), involucrum (blue), cnidoband (orange), elastic strands (pink), terminal structures (yellow). Heteroneme nematocysts (stenoteles in C,E,F,G and mastigophores in H,I) are depicted in red for some species. A - *Erenna laciniata*, 10x. B - *Lychnagalma utricularia*, 10x. C - *Agalma elegans*, 10x. D - *Resomia ornicephala*, 10x. E - *Frillagalma vityazi*, 20x. F - *Bargmannia amoena*, 10x. G - *Cordagalma* sp., reproduced from Carré 1968. H - *Lilyopsis fluoracantha*, 20x. I - *Abylopsis tetragona*, 20x.

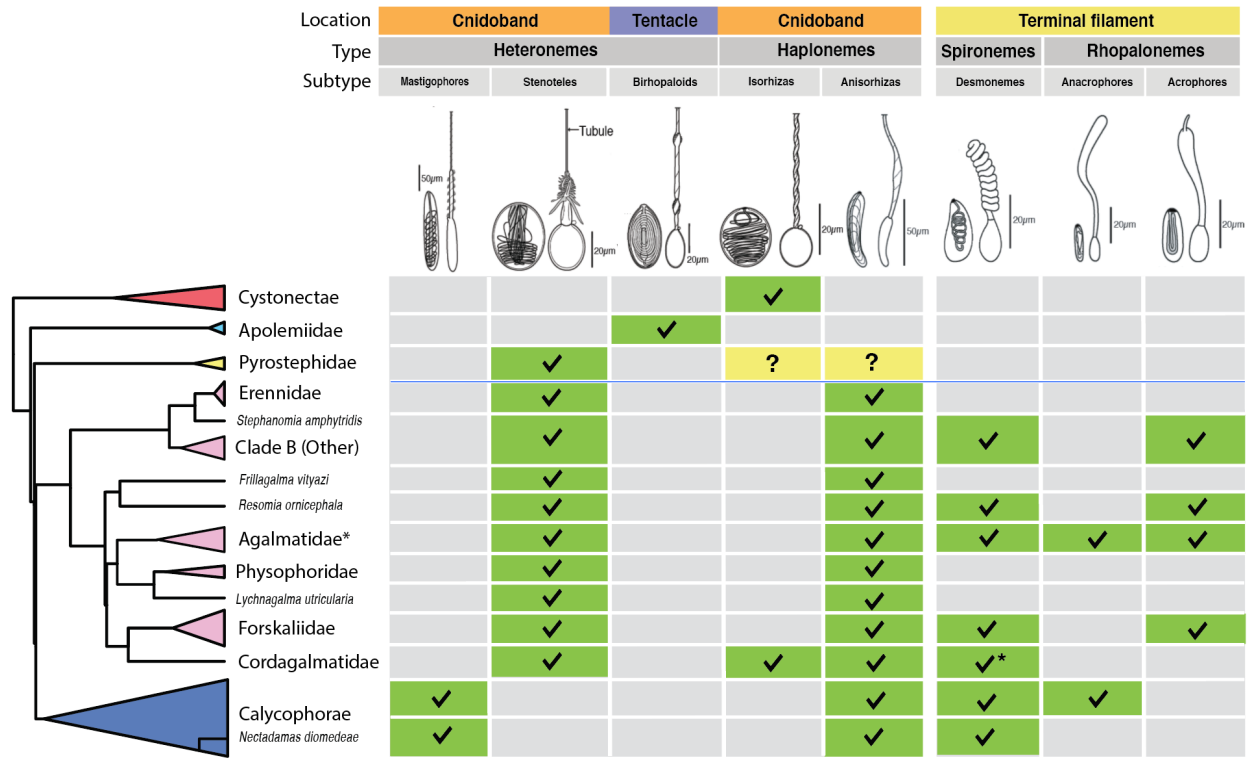


Figure 3: Phylogenetic distribution of nematocyst types and locations in the zooid across the five major siphonophore clades. Illustrations reproduced with permission from Mapstone 2014. Undischarged capsules to the left, discharged to the right. Tick marks indicate presence, only in some species if accompanied by an asterisk. Question marks indicate that it is currently unknown whether pyrostephid haplonemes belong to the isorhiza or the anisorrhiza subtype.

65 work by adhering to the surface of the prey. While recent descriptive studies have expanded
 66 and confirmed our understanding of this diversity, the evolutionary history of nematocyst type
 67 gain and loss in siphonophores remains unexplored. Thus, here we reconstruct the evolution
 68 of shifts, gains, and losses of nematocyst types, subtypes, and other major categorical traits
 69 that led to the extant diversity we see in siphonophore tentilla.

70 Distantly related organisms that evolved to feed on similar resources often evolve similar
 71 adaptations (17). In (14), we found strong associations between piscivory and haploneme
 72 shape across distantly related siphonophore lineages. These associations could have been
 73 produced by convergent changes in the adaptive optima of these characters. Here we
 74 set out to test this hypothesis using comparative model fitting methods. Analyzing the
 75 diversity of morphological states from a phylogenetic perspective allows us to identify the

76 specific evolutionary processes that gave rise to it. Here we fit and compare a variety of
77 macroevolutionary models to siphonophore tentilla morphology measurement data to identify
78 instances of neutral divergence, stabilizing selection, changes in the speed of evolution,
79 convergent evolution, and paedomorphosis (larval characters present in mature colonies).

80 In (14) we fit discriminant analyses to identify characters that are predictive of feeding guild.
81 These discriminant analyses can be used to generate hypotheses on the diets of ecologically
82 understudied siphonophore species for which we have morphology data. Here we present a
83 Bayesian prediction for the feeding guild of 45 species using the morphological dataset in (14).
84 As mentioned above, tentilla are far from being ornamental shapes and are in fact violently
85 reactive weapons for prey capture (14, 18). While we now have detailed characterizations of
86 tentilla morphologies across many species, the diversity of dynamic performances and their
87 relationships to the undischarged morphologies have not been examined to date. To address
88 this gap, we set out to record high-speed video of the *in vivo* discharge dynamics of several
89 siphonophore species at sea, and compare the kinematic attributes to their morphological
90 characters.

91 Methods

92 All character data and the phylogeny analyzed here were published in (14). We log transformed
93 all the continuous characters that did not pass Shapiro-Wilks normality tests, and used
94 the ultrametric constrained Bayesian time tree in all comparative analyses. When missing
95 data was incorporated as inapplicable states, we removed those species with characters that
96 could not be measured due to technical limitations. We used the feeding guild categories
97 detailed in (14) with one modification: including all *Forskalia* spp. as generalists not only
98 a single *Forskalia* species on the tree after a reinterpretation of the data in (19). In order
99 to characterize the evolutionary history of tentilla morphology, we fitted different models
100 generating the observed data distribution given the phylogeny for each continuous character
101 using the function `fitContinuous` in the R package *geiger* (20). These models include a

102 non-phylogenetic white-noise model (WN), a neutral divergence Brownian Motion model
103 (BM), an early-burst decreasing rate model (EB), and an Ornstein-Uhlenbeck (OU) model
104 with stabilizing selection around a fitted optimum trait value. In the same way as (14) we
105 then ordered the models by increasing parametric complexity (WN, BM, EB, OU), and
106 compared their corrected Akaike Information Criterion (AICc) scores (21). We used the
107 lowest (best) score using a delta cutoff of 2 units to determine significance relative to the
108 next simplest model (SM10). We calculated model adequacy scores using the R package
109 *arbutus* (22) (SM11). We calculated phylogenetic signals in each of the measured characters
110 using Blomberg's K (23) (SM10). To reconstruct the ancestral character states of nematocyst
111 types and other categorical traits, we use stochastic character mapping (SIMMAP) using the
112 package *phytools* (24).

113 In order to examine the phenotypic integration in the tentillum, we explored the correla-
114 tional structure among continuous characters and among their evolutionary histories using
115 principal component analysis (PCA) and phylogenetic PCA (24). Since the character dataset
116 contains many gaps due to missing characters and inapplicable states, we carried out these
117 analyses on a subset of species and characters that allowed for the most complete dataset.
118 This was done by removing the terminal filament characters (which are only shared by a small
119 subset of species), and then removing species which had inapplicable states for the remaining
120 characters (apolemiids and cystonects). In addition, we obtained the correlations between
121 the phylogenetic independent contrasts (25) using the package *rphylip* (26). We identified
122 four hypothetical modules among the tentillum characters: (1) The tentillum scaffold module
123 – cnidoband length & width, nematocyst row number, pedicle & elastic strand width, tentacle
124 width; (2) the heteroneme module – heteroneme length & width, shafts length & width; (3)
125 the haploneme module – length and width; and (4) the terminal filament module – desmoneme
126 & rhopaloneme length & width. To test and quantify phenotypic integration between these
127 multivariate modules, we used the phylogenetic phenotypic integration test in the package
128 *geomorph* (27).

When looking at the morphospace of species in different feeding guilds, we also used PCA on the complete tentacular character dataset transforming inapplicable states of absent characters to zeros to account for similarity based on character presence/absence. Using these principal components, we examined the occupation of the morphospace across species in different feeding guilds using a phylogenetic MANOVA with the package *geiger* (20) to assess the variation explained, and a morphological disparity test with the package *geomorph* (27) to assess differences in the extent occupied by each guild.

In order to detect and evaluate instances of convergent evolution, we used the package SURFACE (28). This tool identifies OU regimes and their optima given a tree and character data, and then evaluates where the same regime has appeared independently in different lineages. We applied these analyses to the haploneme nematocyst length and width characters as well as to the most complete dataset without inapplicable character states.

In order to generate hypotheses on the diets of siphonophores using tentilla morphology, we used the discriminant analyses of principal components (DAPC) (29) trained in (14) to predict the feeding guilds of species in the dataset for which there are no published feeding observations.

In order to observe the discharge behavior of different tentilla, we recorded high speed footage (1000-3000 fps) of tentillum and nematocyst discharge by live siphonophore specimens (26 species) using a Phantom Miro 320S camera mounted on a stereoscopic microscope. We mechanically elicited tentillum and nematocyst discharge using a fine metallic pin. We used the Phantom PCC software to analyze the footage. For the 10 species recorded, we measured total cnidoband discharge time (ms), heteroneme filament length (μm), and discharge speeds (mm/s) for cnidoband, heteronemes, haplonemes, and heteroneme shafts when possible (data available in the Dryad repository).

153 **Results**

154 *Evolutionary history of tentillum morphology* – In (14), we produced the most speciose
155 siphonophore molecular phylogeny to date, while incorporating the most recent findings
156 in siphonophore deep node relationships. This phylogeny revealed for the first time that
157 the genus *Erenna* is the sister to *Stephanomia amphytridis*. *Erenna* and *Stephanomia* bear
158 the largest tentilla among all siphonophores, thus their monophyly indicates that there was
159 a single evolutionary transition to giant tentilla. Siphonophore tentilla range in size from
160 ~30 µm in some *Cordagalma* specimens to 2-4 cm in *Erenna* species, and up to 8 cm in
161 *Stephanomia amphytridis* (10). Most siphonophore tentilla measure between 175 and 1007
162 µm (1st and 3rd quartiles), with a median of 373 µm. The extreme gain of tentillum size in
163 this newly found clade may have important implications for access to large prey size classes
164 such as adult deep-sea fishes.

165 Siphonophore tentilla are defined as lateral, monostichous evaginations of the tentacle
166 (including its gastrovascular lumen), armed with epidermal nematocysts (11). The buttons on
167 *Physalia* tentacles were not traditionally regarded as tentilla, but (8) and our observations (13),
168 confirm that the buttons contain evaginations of the gastrovascular lumen, thus satisfying all
169 the criteria for the definition. In this light, and given that most Cystonectae bear conspicuous
170 tentilla, we conclude (in agreement with (13) and (14)) that tentilla were present in the most
171 recent common ancestor of all siphonophores, and secondarily lost twice, once in *Apolemia* and
172 again in *Bathyphysa conifera*. In order to gain a broad perspective on the evolutionary history
173 of tentilla, we reconstructed the phylogenetic positions of the main categorical character
174 shifts using stochastic character mapping (SM1-9) and summarized in (Fig. 4). Some of
175 these characters include the gain and loss of nematocyst types.

176 We assume that haploneme nematocysts are ancestrally present in siphonophore tentacles
177 since they are present in the tentacles of many other hydrozoans (15). Haplonemes are
178 toxin-bearing open-ended nematocysts characterized by the lack of a shaft preceding the
179 tubule. Two subtypes are found in siphonophores: the isorhizas of homogeneous tubule

width, and the anisorhizas with a slight bulking of the tubule near the base. In Cystonectae, haplonemes diverged into spherical isorhizas of two size classes. There is one size of haplonemes in Codonophora, which consist of elongated anisorhizas. Haplonemes were likely lost in the tentacles of *Apolemia* but retained as spherical isorhizas in other *Apolemia* tissues (30). While heteronemes exist in other tissues of cystonects, they appear in the tentacles of codonophorans exclusively, as birhopaloids in *Apolemia*, stenoteles in eucladophoran physonects, and microbasic mastigophores in calycophorans. The four nematocyst types unique to siphonophores appear in two events in the phylogeny (Fig. 4): birhopaloids arose in the stem to *Apolemia*, while rhopalonemes (acrophore and anacrophore) and homotrichous anisorhizas arose in the stem to Tendiculophora.

Nematocyst type gain and loss is also associated with prey capture functions. For example, the loss of desmonemes and rhopalonemes in piscivorous *Erenna*, retaining solely the penetrant (and venom injecting) anisothizas and stenoteles (two size classes) is reminiscent of the two size classes of penetrant isorhizas in the fish-specialist cystonects. Moreover, with the gain of anisorhizas, desmonemes, and rhopalonemes, the Tendiculophora gained versatility in entangling and adhesive functions of the cnidoband and terminal filament, which may have allowed their feeding niches to diversify. Part of the effectiveness of calycophoran cnidobands at entangling crustaceans may be attributed to the subspecialization of their heteronemes. These shifted from the ancestral penetrating stenotele to the microbasic mastigophore (or eurytele in some species) with a long barmed shaft with many long spines. This heteroneme subtype could be better at interlocking with the setae of crustacean legs and antennae.

In those species that have a functional terminal filament, the desmonemes and rhopalonemes play a fundamental role in the first stages of adhesion of the prey. In many species, the tugs of the struggling prey on the terminal filament trigger the cnidoband discharge (18). The adhesive terminal filament has been lost several times in the Euphysonectae (*Frillagalma*, *Lychnagalma-Physophora*, *Erenna*, and some species of *Cordagalma*). In these species, we hypothesize that a different trigger mechanism is at play, possibly involving the

207 prey actively biting or grasping the tentillum or lure.

208 The clades defined in (14) are characterized by unique evolutionary innovations in their
209 tentilla. The clade Eucladophora (containing Pyrostephidae, Euphysonectae, and Caly-
210 cophorae) encompasses all of the extant Siphonophore species (178 of 186) except Cystonects
211 and *Apolemia*. Innovations that arose along the stem of this group include spatially seg-
212 regated heteroneme and haploneme nematocysts, terminal filaments, and elastic strands
213 (Fig. 4). Pyrostephids evolved a unique bifurcation of the axial gastrovascular canal of
214 the tentillum known as the “saccus” (11). The stem to the clade Tendiculophora (clade
215 containing Euphysonectae and Calycophorae) subsequently acquired further novelties such
216 as the desmoneme and rhopaloneme (acrophore subtype ancestral) nematocysts on the
217 terminal filament (Fig. 4), which bears no other nematocyst type. These are arranged
218 in sets of 2 parallel rhopalonemes for each single desmoneme (31, 32). The involucrum is
219 an expansion of the epidermal layer that can cover part or all of the cnidoband (Fig. 2).
220 This structure, together with differentiated larval tentilla, appeared in the stem branch to
221 Clade A physonects. Calycophorans evolved novelties such as larger desmonemes at the
222 distal end of the cnidoband, pleated pedicles with a “hood” (here considered homologous
223 to the involucrum) at the proximal end of the tentillum, anacrophore rhopalonemes, and
224 microbasic mastigophore-type heteronemes. While calycophorans have diversified into most
225 of the extant described siphonophore species (108 of 186), their tentilla have not undergone
226 any major categorical gains or losses since their most recent common ancestor. Nonetheless,
227 they have evolved a wide variation in nematocyst and cnidoband sizes. Ancestrally (and
228 retained in most prayomorphs and hippopodids), the calycophoran tentillum is recurved
229 where the proximal and distal ends of the cnidoband are close together. Diphyomorph tentilla
230 are slightly different in shape, with straighter cnidobands.

231 *Evolution of tentillum and nematocyst characters* – Most (74%) characters present a
232 significant phylogenetic signal, yet only total nematocyst volume, haploneme length, and
233 heteroneme-to-cnidoband length ratio had a phylogenetic signal with K larger than 1. Total

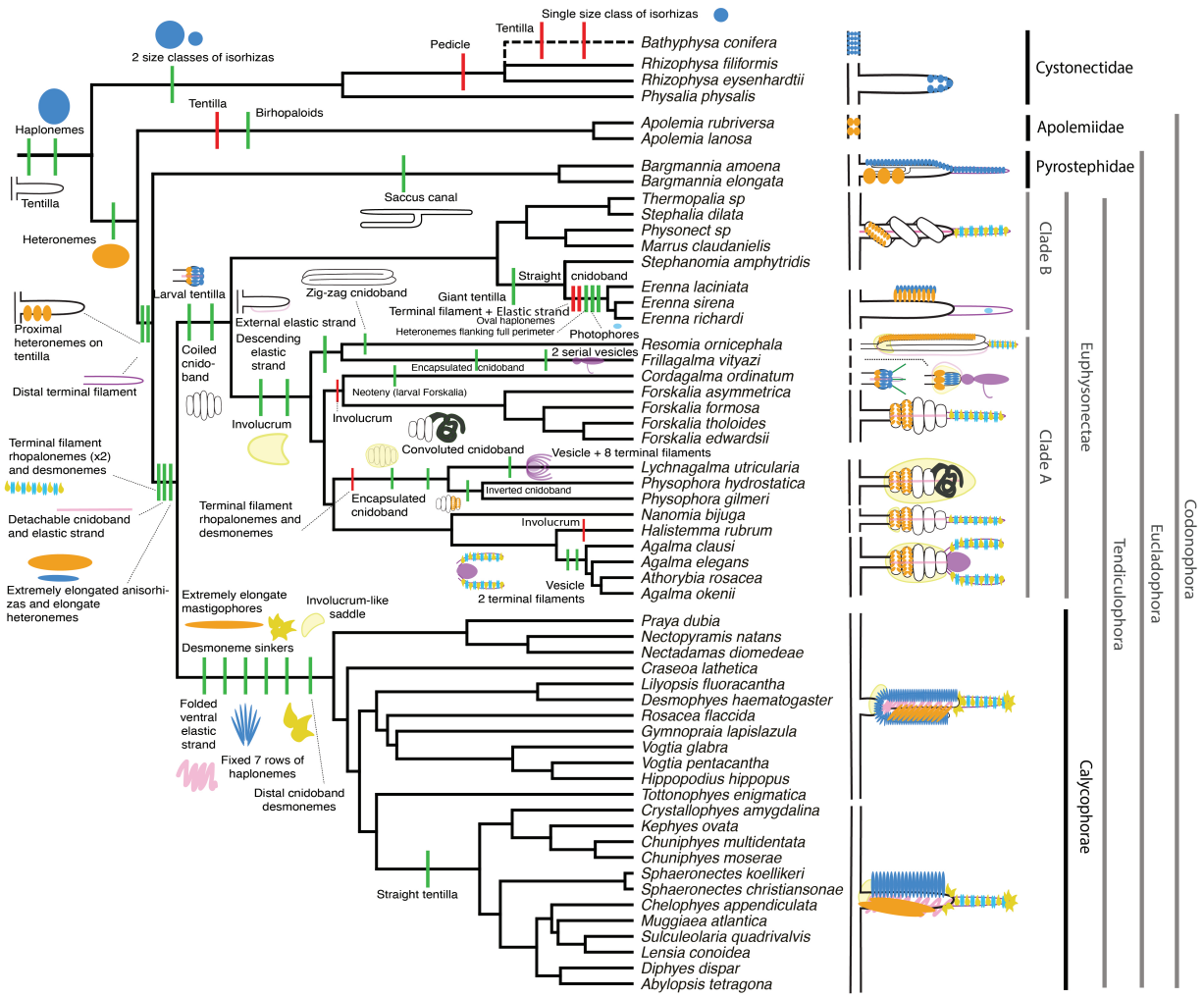


Figure 4: Siphonophore cladogram with the main categorical character gains (green) and losses (red) mapped. Some branch lengths were modified from the Bayesian chronogram to improve readability. The main visually distinguishable tentillum types are sketched next to the species that bear them, showing the location and arrangement of the main characters. In large, complex-shaped euphysonect tentilla, haplonemes were omitted for simplification. The hypothesized phylogenetic placement of the rhizophysid *Bathyphysa conifera*, for which no molecular data are yet available, was added manually (dashed line).

²³⁴ nematocyst volume and cnidoband-to-heteroneme length ratio showed strongly conserved
²³⁵ phylogenetic signals. The majority (67%) of characters were best fitted by BM models,
²³⁶ indicating a history of neutral constant divergence. We did not find any relationship
²³⁷ between phylogenetic signal and specific model support, where characters with high and low
²³⁸ phylogenetic signal were broadly distributed among the best fitted for each model. One-
²³⁹ third of the characters measured in (14) did not recover significant support for any of the
²⁴⁰ phylogenetic models tested, indicating they are either not phylogenetically conserved, or
²⁴¹ they evolved under a complex evolutionary process not represented among the models tested
²⁴² (SM10). Haploneme nematocyst length was the only character with support for an EB model
²⁴³ of decreasing rate of evolution with time. No character had support for a single-optimum OU
²⁴⁴ model (when not informed by feeding guild regime priors). The model adequacy tests (SM11)
²⁴⁵ indicate that many characters may have a relationship between the states and the rates of
²⁴⁶ evolution (Sasr) not captured in the basic models compared here, accompanied by a signal
²⁴⁷ of unaccounted rate heterogeneity (Cvar). No characters show significant deviations in the
²⁴⁸ overall rate of evolution estimated (Msig). Some characters show a perfect fit (no significant
²⁴⁹ deviations across all metrics) under BM evolution, such as heteroneme shape, length, width
²⁵⁰ & volume, haploneme width & SA/V, tentacle width and pedicle width. Haploneme row
²⁵¹ number and rhopaloneme shape have significant deviations across four metrics, indicating
²⁵² that BM (best model) is a poor fit. These characters likely evolved under complex models
²⁵³ which would require many more data points than we have available to fit with accuracy.

²⁵⁴ *Evolution of nematocyst shape* – The greatest evolutionary change in haploneme nema-
²⁵⁵ tocyst shape occurred in a single shift towards elongation in the stem of Tendiculophora,
²⁵⁶ which contains the majority of described siphonophore species, *i.e.* all siphonophores other
²⁵⁷ than Cystonects, *Apolemia*, and Pyrostephidae. There is one secondary return to more
²⁵⁸ oval, less elongated haplonemes in *Erenna*, but it does not reach the sphericity present
²⁵⁹ in Cystonectae or Pyrostephidae (Fig. 6). Heteroneme evolution presents a less discrete
²⁶⁰ evolutionary history. Tendiculophora evolved more elongate heteronemes along the stem, but

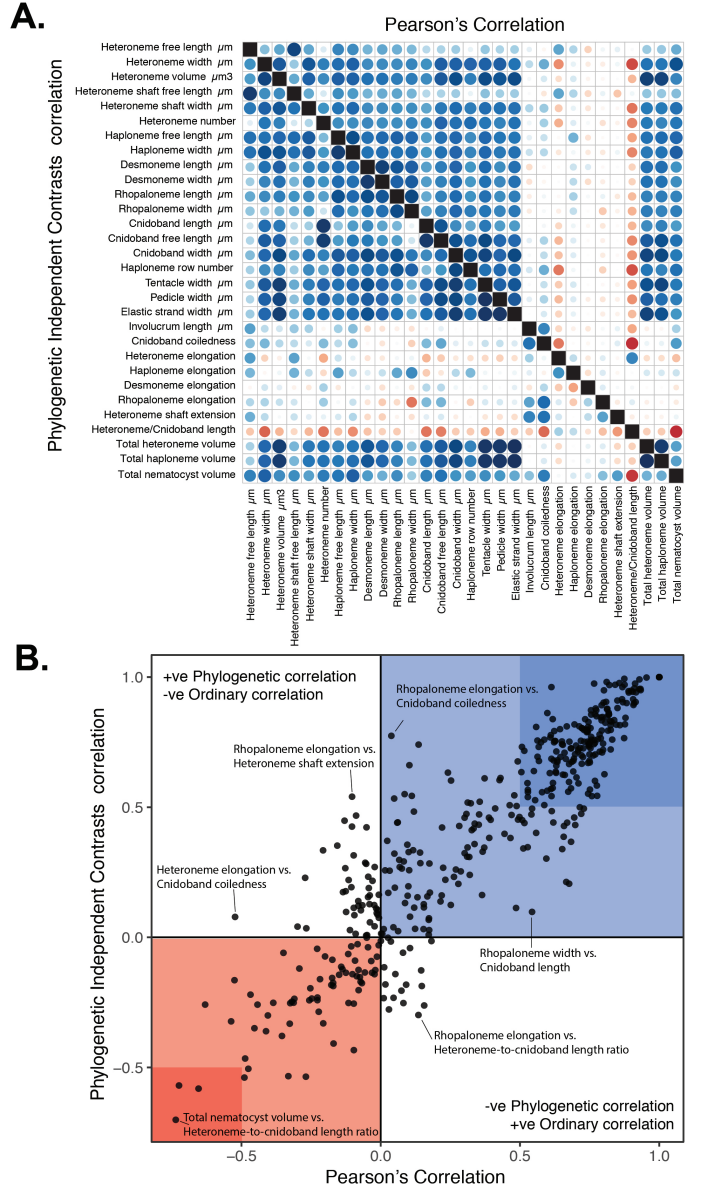


Figure 5: A. Correlogram showing strength of ordinary (upper triangle) and phylogenetic (lower triangle) correlations between characters. Both size and color of the circles indicate the strength of the correlation (R^2). B. Scatterplot of phylogenetic correlation against ordinary correlation showing a strong linear relationship ($R^2 = 0.92$, 95% confidence between 0.90 and 0.93). Light red and blue boxes indicate congruent negative and positive correlations respectively. Darker red and blue boxes indicate strong (<-0.5 or >0.5) negative and positive correlation coefficients respectively.

261 the difference between theirs and other siphonophores' is much smaller than the variation
262 in shape within Tendiculophora, bearing no phylogenetic signal within this clade. In this
263 clade, the evolution of heteroneme shape has diverged in both directions, and there is no
264 correlation with haploneme shape (Fig. 6), which has remained fairly constant (elongation
265 between 1.5 and 2.5).

266 Haploneme and heteroneme shape share 21% of their variance across extant values, and
267 53% of the variance in their shifts along the branches of the phylogeny. However, much of
268 this correlation is due to the sharp contrast between Pyrostephidae and their sister group
269 Tendiculophora. We searched for regime shifts in the evolution of haploneme nematocyst
270 shape characters using SURFACE (28). SURFACE identified eight distinct OU regimes in
271 the evolutionary history of haploneme length and width (Fig. 9A). The different regimes are
272 located (1) in cystonects, (2) in most of Tendiculophora, (3) in most diphyomorphs, (4) in
273 *Cordagalma ordinatum*, (5) in *Stephanomia amphytridis*, (6) in pyrostephids, (7) in *Diphyes*
274 *dispar* + *Abylopsis tetragona*, and (8) in *Erenna* spp.

275 *Phenotypic integration of the tentillum* – Phenotypically integrated structures maintain
276 evolutionary correlations between its constituent characters. Of the phylogenetic correlations
277 (Fig. 5a, lower triangle), 81.3% were positive and 18.7% were negative, while of the ordinary
278 correlations (Fig. 5a, upper triangle) 74.6% were positive and 25.4% were negative. Half
279 (49.9%) of phylogenetic correlations were >0.5 , while only 3.6% are < -0.5 . Similarly, among
280 the correlations across extant species, 49.1% were >0.5 and only 1.5% were < -0.5 . In
281 addition, we found that 13.9% of character pairs had opposing phylogenetic and ordinary
282 correlation coefficients. Just 4% have negative phylogenetic and positive ordinary correlations
283 (such as rhopaloneme elongation ~ heteroneme-to-cnidoband length ratio and haploneme
284 elongation, or haploneme elongation ~ heteroneme number), and only 9.9% of character pairs
285 had positive phylogenetic correlation yet negative ordinary correlation (such as heteroneme
286 elongation ~ cnidoband convolution and involucrum length, or rhopaloneme elongation with
287 cnidoband length). These disparities could be explained by Simpson's paradox (33): the

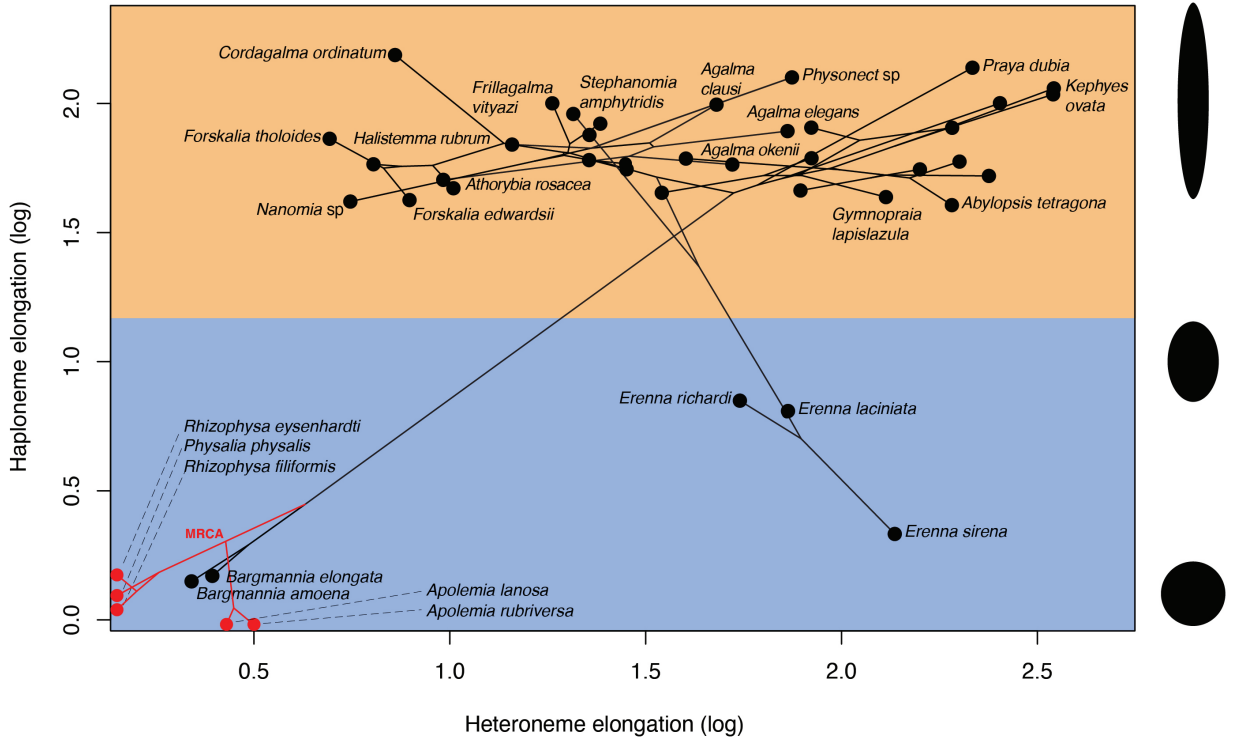


Figure 6: Phylomorphospace showing haploneme and heteroneme elongation (log scaled). Orange area delimits rod-shaped haplonemes, the blue area covers oval and round-shaped haplonemes. Smaller dots and lines represent phylogenetic relationships and ancestral states of internal nodes under BM. Species nodes in red lack either haplonemes or heteronemes, and their values are projected onto the axis of the nematocyst type they bear. Cystonects have no tentacle heteronemes and are projected onto the haploneme axis. Apolemiids have no tentacle haplonemes and are projected onto the heteroneme axis.

reversal of the sign of a relationship when a third variable (or a phylogenetic topology (34)) is considered. However, no character pair had correlation coefficient differences larger than 0.64 between ordinary and phylogenetic correlations (heteroneme shaft extension ~ rhopaloneme elongation has a Pearson's correlation of 0.10 and a phylogenetic correlation of -0.54). Rhopaloneme elongation shows the most incongruencies between phylogenetic and ordinary correlations with other characters. The phenotypic integration test showed significant integration signal between all modules, tentillum and haploneme modules sharing the greatest regression coefficient (SM12).

In the non-phylogenetic PCA morphospace using only characters derived from simple measurements (Fig. 7), PC1 (aligned with tentillum and tentacle size) explained 69.3% of the variation in the tentillum morphospace, whereas PC2 (aligned with heteroneme length, heteroneme number, and haploneme arrangement) explained 13.5%. In a phylogenetic PCA, 63% of the evolutionary variation in the morphospace is explained by PC1 (aligned with shifts in tentillum size), while 18% is explained by PC2 (aligned with shifts in heteroneme number and involucrum length).

Morphospace occupation – In order to examine the occupation structure of the morphospace across all siphonophore species in the dataset, we cast a PCA on the data after transforming inapplicable states (due to absence of character) to zeroes. This allows us to accommodate species with many missing characters (such as cystonects or apolemiids), and to account for common absences as morphological similarities. In this ordination, PC1 (aligned with cnidoband size) explains 47.45% of variation and PC2 (aligned with heteroneme volume and involucrum length) explains 16.73% of variation . When superimposing feeding guilds onto the morphospace (Fig. 8), we find that the morphospaces of each feeding guild are only slightly overlapping in PC1 and PC2. A phylogenetic MANOVA showed that feeding guilds explain 27.63% of variance across extant species (p value < 0.000001), and 20.97% of the variance in the tree species accounting for phylogeny, an outcome significantly distinct from the expectation under neutral evolution (p -value = 0.0196). In addition, a morphological

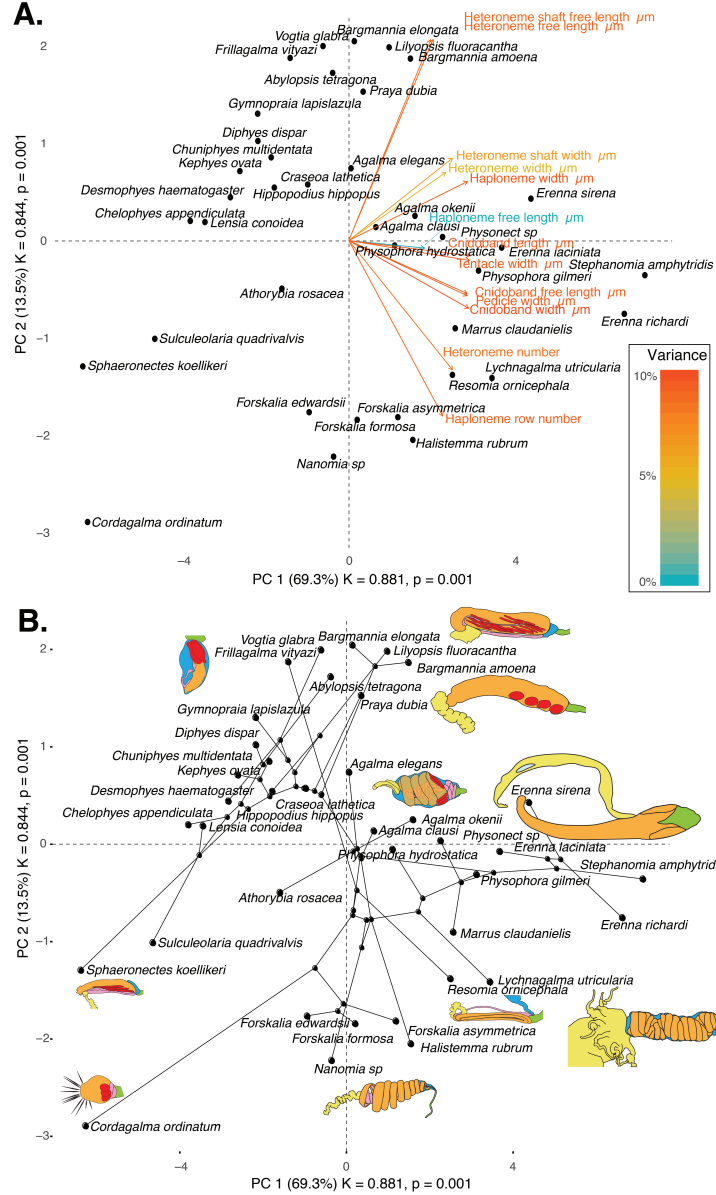


Figure 7: Phylomorphospace of the simple-measurement continuous characters principal components, excluding ratios and composite characters. A. Variance explained by each variable in the PC1-PC2 plane. Axis labels include the phylogenetic signal (K) for each component and p-value. B. Phylogenetic relationships between the species points distributed in that same space.

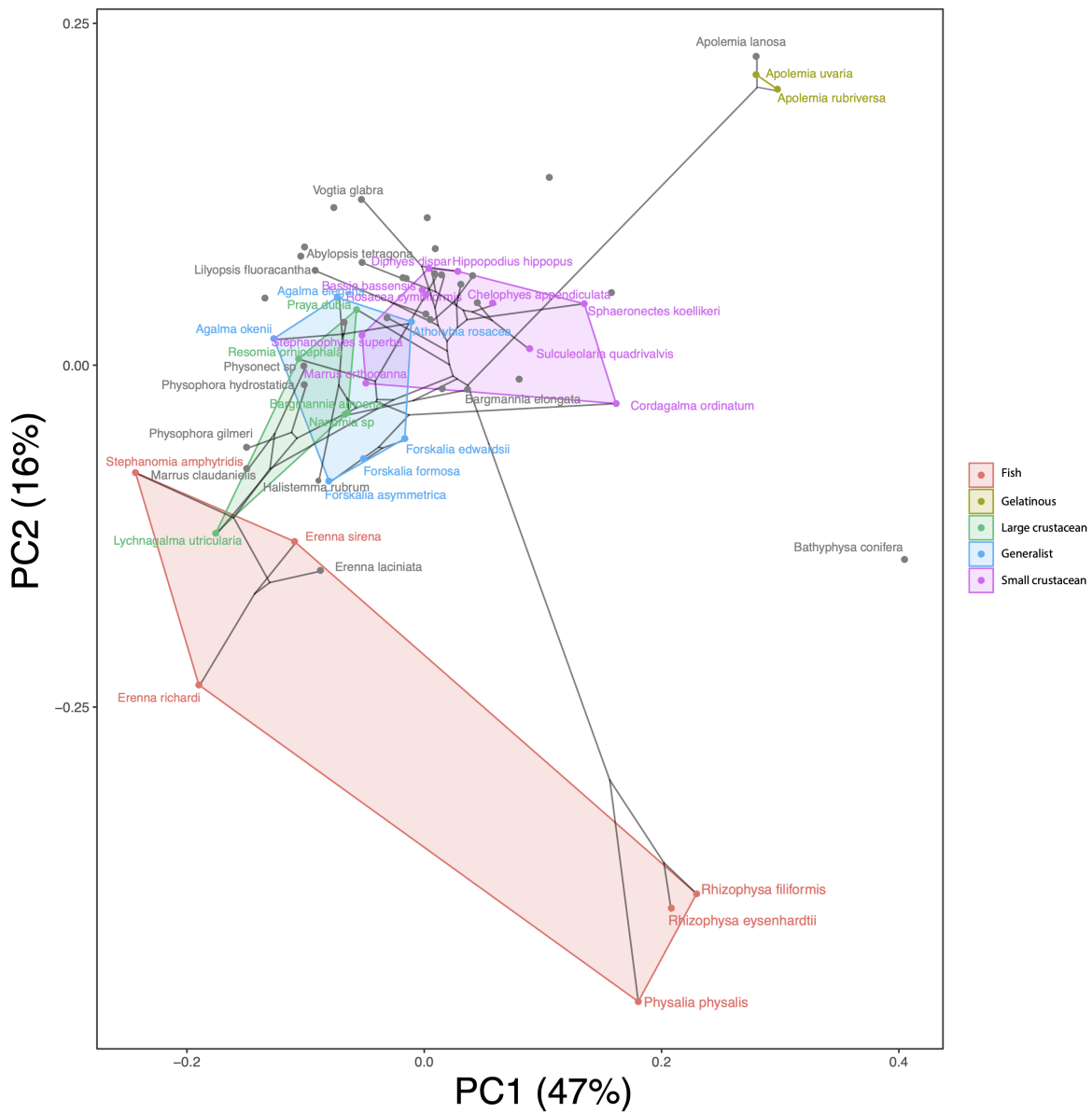


Figure 8: Phylomorphospace showing PC1 and PC2 from a PCA of continuous morphological characters with inapplicable states transformed to zeroes, overlapped with polygons conservatively defining the space occupied by each feeding guild. Lines between species coordinates show the phylogenetic relationships between them.

³¹⁵ disparity analysis accounting for phylogenetic structure shows that the morphospace of fish
³¹⁶ specialists is significantly broader than that of generalists and other specialists. This is due to
³¹⁷ the large morphological disparities between cystonects and piscivorous euphysonects. There
³¹⁸ are no significant differences among the morphospace disparities of the other feeding guilds.

³¹⁹ *Convergent evolution* – Convergence is a widespread evolutionary phenomenon where
³²⁰ distantly related clades independently evolve similar phenotypes. When the dimensionality of
³²¹ the state space is small as it is in tentilla morphology, convergence is more likely given the same
³²² amount of evolutionary change. Using the package SURFACE (28), we identified convergence
³²³ in haploneme nematocyst shape and in morphospace position. In (14), we identified haploneme
³²⁴ nematocyst shape as one of the traits associated with the convergent evolution of piscivory.
³²⁵ Here we find that indeed wider haploneme nematocysts have convergently evolved in the
³²⁶ piscivore cytonects and *Erenna* spp. (Fig. 9A). Extremely narrow haplonemes have also
³²⁷ evolved convergently in *Cordagalma ordinatum* and copepod specialist calycophorans such as
³²⁸ *Sphaeronectes koellikeri*. When integrating many traits into a couple principal components, we
³²⁹ find two distinct convergences between euphysonects and calycophorans with a reduced prey
³³⁰ capture apparatus. Those convergences are between *Frillagalma vityazi* and calycophorans,
³³¹ and once again between *Cordagalma ordinatum* and *Sphaeronectes koellikeri* (Fig. 9B).

³³² *Functional morphology of tentillum and nematocyst discharge* – Tentillum and nematocyst
³³³ discharge high speed videos and measurements are available in the Dryad repository. While
³³⁴ the sample sizes of these measurements were insufficient to draw reliable statistical results
³³⁵ at a phylogenetic level, we did observe patterns that may be relevant to their functional
³³⁶ morphology. For example, cnidoband length is strongly correlated with discharge speed (p
³³⁷ value = 0.0002). This explains much of the considerable difference between euphysonect and
³³⁸ calycophoran tentilla discharge speeds (average discharge speeds: 225.0mm/s and 41.8mm/s
³³⁹ respectively; t-test p value = 0.011), since the euphysonects have larger tentilla than the
³⁴⁰ calycophorans among the species recorded. In addition, we observed that calycophoran
³⁴¹ haploneme tubules fire faster than those of euphysonects (t-test p value = 0.001). Haploneme

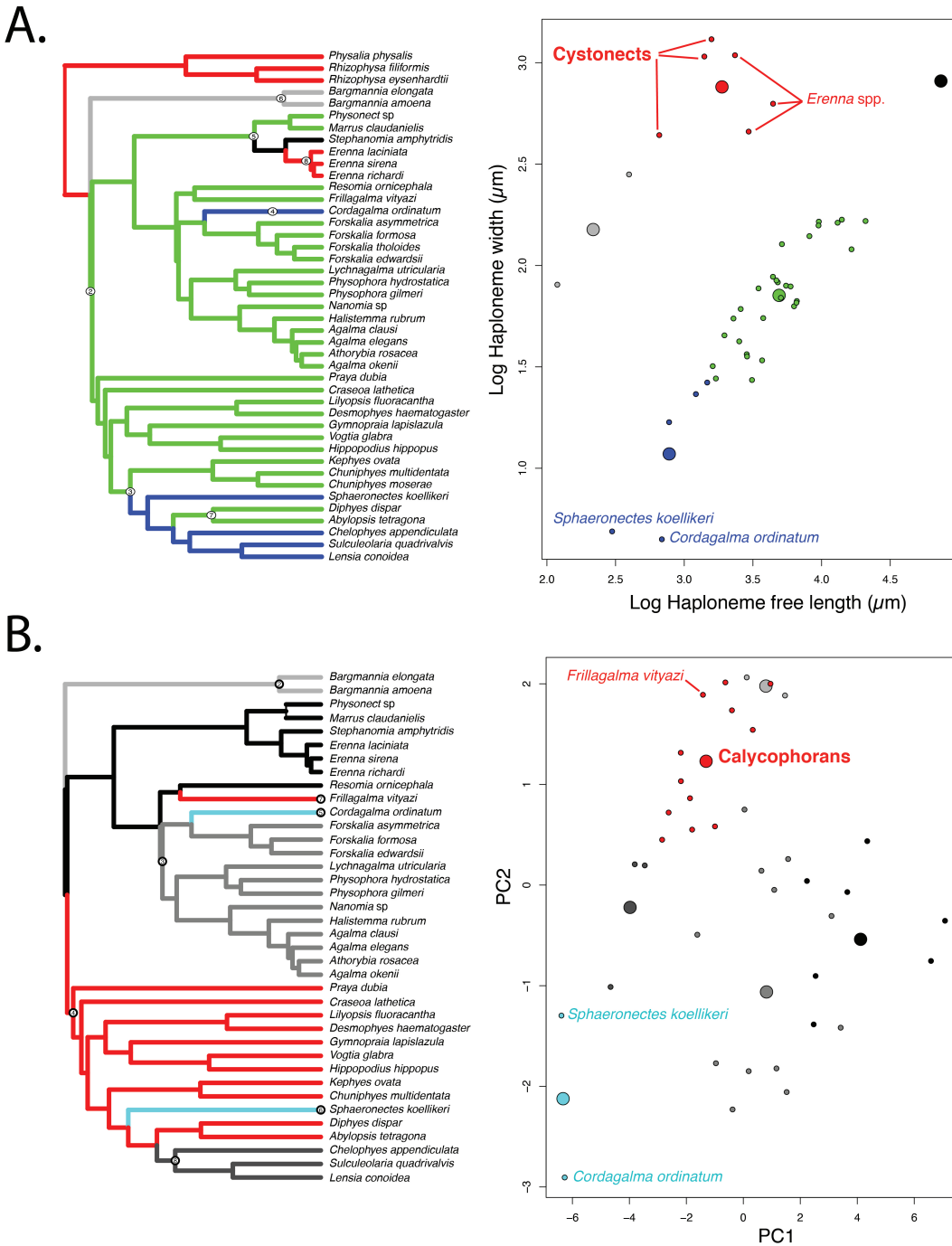


Figure 9: SURFACE plots showing convergent evolutionary regimes modelled under OU for (A) haploneme nematocyst length & width, and (B) for PC1 & 2 of all continuous characters with the exception of terminal filament nematocysts, and removing taxa with inapplicable character states. Node numbers on the tree label different regimes, regimes of the same color are identified as convergent. Small circles on the scatterplots indicate species values, large circles indicate the average position of the OU optima (θ) for a given combination of convergent regimes.

³⁴² nematocysts discharge 2.8x faster than heteroneme nematocysts (t-test p value = 0.0012).

³⁴³ Finally, we observed that the stenoteles of the Euphysonectae discharge a helical filament

³⁴⁴ that “drills” itself through the medium it penetrates as it everts.

³⁴⁵ *Generating dietary hypotheses using tentillum morphology* – For many siphonophore species,
³⁴⁶ no feeding observations have yet been published. To help bridge this gap of knowledge,
³⁴⁷ we generated hypotheses about the diets of these understudied siphonophores based on
³⁴⁸ their known tentacle morphology using one of the linear discriminant analyses of principal
³⁴⁹ components (DAPC) fitted in (14). This provides concrete predictions to be tested in
³⁵⁰ future work and helps extrapolate our findings to many poorly known species that are
³⁵¹ extremely difficult to collect and observe. The discriminant analysis for feeding guild (7
³⁵² principal components, 4 discriminants) produced 100% discrimination, and the highest loading
³⁵³ contributions were found for the characters (ordered from highest to lowest): Involutrum
³⁵⁴ length, heteroneme volume, heteroneme number, total heteroneme volume, tentacle width,
³⁵⁵ heteroneme length, total nematocyst volume, and heteroneme width. We used the predictions
³⁵⁶ from this discriminant function to generate hypotheses about the feeding guild of 45 species
³⁵⁷ in the morphological dataset. This extrapolation predicts that two other *Apolemia* species are
³⁵⁸ gelatinous prey specialists like *Apolemia rubriversa*, and predicts that *Erenna laciniata* is a
³⁵⁹ fish specialist like *Erenna richardi*. When predicting soft- and hard-bodied prey specialization,
³⁶⁰ the DAPC achieved 90.9% discrimination success, only marginally confounding hard-bodied
³⁶¹ specialists with generalists (SM13). The main characters driving this discrimination are
³⁶² involutrum length, heteroneme number, heteroneme volume, tentacle width, total nematocyst
³⁶³ volume, total haploneme volume, elastic strand width, and heteroneme length.

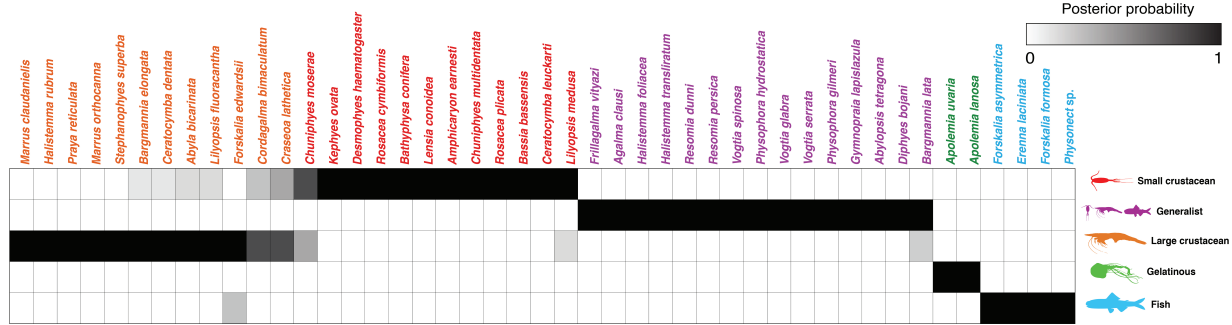


Figure 10: Hypothetical feeding guilds for siphonophore species predicted by a 6 PCA DAPC. Cell darkness indicates the posterior probability of belonging to each guild. Training data set transformed so inapplicable states are computed as zeroes. Species ordered and colored according to their predicted feeding guild.

364 Discussion

365 *On the evolution of tentilla morphology* – The evolutionary rate covariance results in (14)
 366 indicate that tentilla are not only phenotypically integrated (with widespread evolutionary
 367 correlations across structures) but also show patterns of evolutionary modularity, where
 368 different sets of characters appear to evolve in stronger correlations among each other
 369 than with other characters (35). This may be indicative of the underlying genetic and
 370 developmental dependencies among closely homologous nematocyst types (such as desmonemes
 371 and rhopalonemes) and structures. The rate covariance results are congruent with the
 372 evolutionary correlations we found (Fig. 5). In addition, these evolutionary modules point
 373 to hypothetical functional modules. For example, the coiling degree of the cnidoband and
 374 the extent of the involucrum have correlated rates of evolution, while high-speed videos
 375 show that the involucrum helps direct the whiplash of the uncoiling cnidoband distally
 376 (towards the prey). The clade Tendiculophora contains far more species than its relatives
 377 Cystonectae, Apolemiidae, and Pyrostephidae. An increase in clade richness and ecological
 378 diversification can be triggered by a ‘key innovation’ (36). The evolutionary innovation of the
 379 Tendiculophora tentilla with shooting cnidobands and modular regions may have facilitated
 380 further dietary diversification. A specific instance of this may have been the access to the
 381 abundant small crustacean prey such as copepods. The rapid darting escape response of

³⁸² copepods may preclude their capture in siphonophores without shooting cnidobands.

³⁸³ Siphonophore tentilla are beautifully complex and highly diverse. Our analyses show,
³⁸⁴ however, that the siphonophore tentillum morphospace actually has a fairly low extant
³⁸⁵ dimensionality due to having an evolutionary history with many synchronous, correlated
³⁸⁶ changes. This is consistent with strong phenotypic integration where genetic and devel-
³⁸⁷ opmental correlations are maintained by natural selection to preserve a complex function
³⁸⁸ across the wide variety of morphologies present. Since most tentillum characters develop
³⁸⁹ from a common bud (budding tentilla near the base of the tentacle), structural correlations
³⁹⁰ are expected. Similarly, correlations between the features of different nematocyst subtypes
³⁹¹ within a species are also expected given their common evolutionary and developmental origin
³⁹² (37, 38). However, we also found correlations between nematocyst and tentillum characters.
³⁹³ Siphonophore tentacle nematocysts (in their cnidocytes) are not produced nor matured in the
³⁹⁴ developing tentillum. These cnidocytes are produced by dividing cnidoblasts in the basigaster
³⁹⁵ (basal swelling of the gastrozooid). Once the cnidocytes have assembled the nematocyst, they
³⁹⁶ migrate outward along the tentacle (39) and position themselves in the tentillum according
³⁹⁷ to their type and size (31). Thus, the developmental programs that produce the observed
³⁹⁸ nematocyst morphologies are spatially separated from those producing the tentillum mor-
³⁹⁹ phologies. Therefore, we hypothesize the genetic correlations and phenotypic integration
⁴⁰⁰ between tentillum and nematocyst characters are maintained through natural selection on
⁴⁰¹ separate regulatory networks, out of the necessity to work together and meet the spatial,
⁴⁰² mechanical, and functional constraints of their prey capture behavior.

⁴⁰³ *Heterochrony and convergence in the evolution of tentilla with diet* - In addition to
⁴⁰⁴ identifying shifts in prey type, (14) revealed the specific morphological changes in the prey
⁴⁰⁵ capture apparatus associated with these changes. Copepod-specialized diets have evolved
⁴⁰⁶ independently in *Cordagalma* and some calycophorans. These evolutionary transitions
⁴⁰⁷ happened together with transitions to smaller tentilla with fewer and smaller cnidoband
⁴⁰⁸ nematocysts. We found that these morphological transitions evolved convergently in these

409 taxa. Tentilla are expensive single-use structures (18), therefore we would expect that
410 specialization in small prey would beget reductions in the size of the prey capture apparatus
411 to the minimum required for the ecological performance. Such a reduction in size would
412 require extremely fast rates of trait evolution in an ordinary scenario. However, *Cordagalma*'s
413 tentilla strongly resemble the larval tentilla (only found in the first-budded feeding body of
414 the colony) of their sister genus *Forskalia*. This indicates that the evolution of *Cordagalma*
415 tentilla could be a case of paedomorphic heterochrony associated with predatory specialization
416 on smaller prey. This developmental shift may have provided a shortcut for the evolution of
417 a smaller prey capture apparatus.

418 Our work identifies yet another novel example of convergent evolution. The region of the
419 tentillum morphospace (Fig. 7 & Fig. 9B) occupied by calycophorans was independently (and
420 more recently) occupied by the physonect *Frillagalma vityazi*. Like calycophorans, *Frillagalma*
421 tentilla have small C-shaped cnidobands with a few rows of anisorhizas. Unlike calycophorans,
422 they lack paired elongate microbasic mastigophores. Instead, they bear exactly three oval
423 stenoteles, and their cnidobands are followed by a branched vesicle, unique to this genus.
424 Their tentillum morphology is very different from that of other related physonects, which tend
425 to have long, coiled, cnidobands with many paired oval stenoteles. Our SURFACE analysis
426 clearly indicates a regime convergence in the cnidoband morphospace between *Frillagalma*
427 and calycophorans (Fig. 9B). Most studies on calycophoran diets have reported their prey to
428 be primarily composed of small crustaceans, such as copepods or ostracods (19, 40). The
429 diet of *Frillagalma vityazi* is unknown, but this morphological convergence suggests that they
430 evolved to capture similar kinds of prey. The DAPCs in (14) predict that *Frillagalma* has a
431 generalist niche with both soft and hard-bodied prey, including copepods.

432 *Evolution of nematocyst shape* – A remarkable feature of siphonophore haplonemes is
433 that they are outliers to all other Medusozoa in their surface area to volume relationships,
434 deviating significantly from sphericity (41). This suggests a different mechanism for their
435 discharge that could be more reliant on capsule tension than on osmotic potentials (42), and

436 strong selection for efficient nematocyst packing in the cnidoband (31, 41). Our results show
437 that Codonophora underwent a shift towards elongation and Cystonectae towards sphericity,
438 assuming the common ancestor had an intermediate state. Since we know that the haplonemes
439 of other hydrozoan outgroups are generally spheroid, it is more parsimonious to assume that
440 cystonects are simply retaining this ancestral state. Later, we observe a return to more
441 rounded (ancestral) haplonemes in *Erenna*, concurrent with a secondary gain of a piscivorous
442 trophic niche, like that exhibited by cystonects. Our SURFACE analysis shows that this
443 transition to roundness is convergent with the regime occupied by cystonects (Fig. 9A).
444 Purcell (40) showed that haplonemes have a penetrating function as isorhizas in cystonects
445 and an adhesive function as anisorhizas in Tendiculophora. It is no coincidence that the two
446 clades that have converged to feed primarily on fish have also converged morphologically
447 toward more compact haplonemes. Isorhizas in cystonects are known to penetrate the skin of
448 fish during prey capture, and to deliver the toxins that aid in paralysis and digestion (43).
449 *Erenna*'s anisorhizas are also able to penetrate human skin and deliver a painful sting (4)
450 (and pers. obs.), a common feature of piscivorous cnidarians like the Portuguese man-o-war
451 or box jellies.

452 The implications of these results for the evolution of nematocyst function are that an
453 innovation in the discharge mechanism of haplonemes may have occurred during the main shift
454 to elongation. Elongate nematocysts can be tightly packed into cnidobands. We hypothesize
455 this may be a Tendiculophora lineage-specific adaptation to packing more nematocysts into a
456 limited tentillum space, as suggested by (31). Thomason (41) hypothesized that smaller, more
457 spherical nematocysts, with a lower surface area to volume ratio, are more efficient in osmotic-
458 driven discharge and thus have more power for skin penetration. The elongated haplonemes
459 of crustacean-eating Tendiculophora have never been observed penetrating their crustacean
460 prey (40), and are hypothesized to entangle the prey through adhesion of the abundant
461 spines to the exoskeletal surfaces and appendages. Entangling requires less acceleration and
462 power during discharge than penetration, as it does not rely on point pressure. In fish-eating

⁴⁶³ cystonects and *Erenna* species, the haplonemes are much less elongated and very effective at
⁴⁶⁴ penetration, in congruence with the osmotic discharge hypothesis. Tendiculophora, composed
⁴⁶⁵ of the clades Euphysonectae and Calycophorae, includes the majority of siphonophore species.
⁴⁶⁶ Within these clades are the most abundant siphonophore species, and a greater morphological
⁴⁶⁷ and ecological diversity is found. We hypothesize that this packing-efficient haploneme
⁴⁶⁸ morphology may have also been a key innovation leading to the diversification of this clade.
⁴⁶⁹ However, other characters that shifted concurrently in the stem of this clade could have been
⁴⁷⁰ equally responsible for their extant diversity.

⁴⁷¹ *Generating hypotheses on siphonophore feeding ecology* – One motivation for our research
⁴⁷² is to understand the links between prey-capture tools and diets so we can generate hypotheses
⁴⁷³ about the diets of predators based on morphological characteristics. Indeed, our discriminant
⁴⁷⁴ analyses were able to distinguish between different siphonophore diets based on morphological
⁴⁷⁵ characters alone. The models produced by these analyses generated testable predictions
⁴⁷⁶ about the diets of many species for which we only have morphological data of their tentacles.
⁴⁷⁷ While the limited dataset used here is informative for generating tentative hypotheses, the
⁴⁷⁸ empirical dietary data are still scarce and insufficient to cast robust predictions. This reveals
⁴⁷⁹ the need to extensively characterize siphonophore diets and feeding habits. In future work, we
⁴⁸⁰ will test these ecological hypotheses and validate these models by directly characterizing the
⁴⁸¹ diets of some of those siphonophore species. Predicting diet using morphology is a powerful
⁴⁸² tool to reconstruct food web topologies from community composition alone. In many of the
⁴⁸³ ecological models found in the literature, interactions among the oceanic zooplankton have
⁴⁸⁴ been treated as a black box (44). The ability to predict such interactions, including those of
⁴⁸⁵ siphonophores and their prey, will enhance the taxonomic resolution of nutrient-flow models
⁴⁸⁶ constructed from plankton community composition data.

487 **Acknowledgements**

488 This work was supported by the Society of Systematic Biologists (Graduate Student Award
489 to A.D.S.); the Yale Institute of Biospheric Studies (Doctoral Pilot Grant to A.D.S.); and
490 the National Science Foundation (Waterman Award to C.W.D., and NSF-OCE 1829835 to
491 C.W.D., S.H.D.H., and C. Anela Choy). A.D.S. was supported by a Fulbright Spain Graduate
492 Studies Scholarship.

493 **References**

- 494 1. Pugh P (1983) *Benthic siphonophores: A review of the family rhodaliidai (siphonophora,
495 physonectae)* (Royal Society).
- 496 2. Pugh P, Harbison G (1986) New observations on a rare physonect siphonophore,
497 lychnagalma utricularia (claus, 1879). *Journal of the Marine Biological Association of the
498 United Kingdom* 66(3):695–710.
- 499 3. Pugh P, Youngbluth M (1988) Two new species of prayine siphonophore (calycophorae,
500 prayidae) collected by the submersibles johnson-sea-link i and ii. *Journal of Plankton Research*
501 10(4):637–657.
- 502 4. Pugh P (2001) A review of the genus erenna bedot, 1904 (siphonophora, physonectae).
503 *BULLETIN-NATURAL HISTORY MUSEUM ZOOLOGY SERIES* 67(2):169–182.
- 504 5. Hissmann K (2005) In situ observations on benthic siphonophores (physonectae: Rho-
505 daliidae) and descriptions of three new species from indonesia and south africa. *Systematics
506 and Biodiversity* 2(3):223–249.
- 507 6. Haddock SH, Dunn CW, Pugh PR (2005) A re-examination of siphonophore terminology
508 and morphology, applied to the description of two new prayine species with remarkable bio-
509 optical properties. *Journal of the Marine Biological Association of the United Kingdom*
510 85(3):695–707.
- 511 7. Dunn CW, Pugh PR, Haddock SH (2005) Marrus claudanielis, a new species of
512 deep-sea physonect siphonophore (siphonophora, physonectae). *Bulletin of Marine Science*

- 513 76(3):699–714.
- 514 8. Bardi J, Marques AC (2007) Taxonomic redescription of the portuguese man-of-war,
515 physalia physalis (cnidaria, hydrozoa, siphonophorae, cystonectae) from brazil. *Iheringia*
516 *Série Zoologia* 97(4):425–433.
- 517 9. Pugh P, Haddock S (2010) Three new species of remosiid siphonophore (siphonophora:
518 Physonectae). *Journal of the Marine Biological Association of the United Kingdom* 90(6):1119–
519 1143.
- 520 10. Pugh P, Baxter E (2014) A review of the physonect siphonophore genera halistemma
521 (family agalmatidae) and stephanomia (family stephanomiidae). *Zootaxa* 3897(1):1–111.
- 522 11. Totton AK, Bargmann HE (1965) *A synopsis of the siphonophora* (British Museum
523 (Natural History)).
- 524 12. Mapstone GM (2014) Global diversity and review of siphonophorae (cnidaria: Hydro-
525 zoa). *PLoS One* 9(2):e87737.
- 526 13. Munro C, et al. (2018) Improved phylogenetic resolution within siphonophora
527 (cnidaria) with implications for trait evolution. *Molecular Phylogenetics and Evolution*.
- 528 14. Damian-Serrano A, Haddock SH, Dunn CW (2019) The evolution of siphonophore
529 tentilla as specialized tools for prey capture. *bioRxiv*:653345.
- 530 15. Mariscal RN (1974) Nematocysts.
- 531 16. Werner B (1965) Die nesselkapseln der cnidaria, mit besonderer berücksichtigung der
532 hydriida. *Helgoländer wissenschaftliche Meeresuntersuchungen* 12(1):1.
- 533 17. Winemiller KO, Fitzgerald DB, Bower LM, Pianka ER (2015) Functional traits,
534 convergent evolution, and periodic tables of niches. *Ecology letters* 18(8):737–751.
- 535 18. Mackie GO, Pugh PR, Purcell JE (1987) Siphonophore Biology. *Advances in Marine*
536 *Biology* 24:97–262.
- 537 19. Purcell J (1981) Dietary composition and diel feeding patterns of epipelagic
538 siphonophores. *Marine Biology* 65(1):83–90.
- 539 20. Harmon LJ, Weir JT, Brock CD, Glor RE, Challenger W (2007) GEIGER: Investi-

- 540 gating evolutionary radiations. *Bioinformatics* 24(1):129–131.
- 541 21. Sugiura N (1978) Further analysts of the data by akaike's information criterion
542 and the finite corrections: Further analysts of the data by akaike's. *Communications in*
543 *Statistics-Theory and Methods* 7(1):13–26.
- 544 22. Pennell MW, FitzJohn RG, Cornwell WK, Harmon LJ (2015) Model adequacy and the
545 macroevolution of angiosperm functional traits. *The American Naturalist* 186(2):E33–E50.
- 546 23. Blomberg SP, Garland T, Ives AR (2003) Testing for phylogenetic signal in comparative
547 data: Behavioral traits are more labile. *Evolution* 57(4):717–745.
- 548 24. Revell LJ (2012) Phytools: An r package for phylogenetic comparative biology (and
549 other things). *Methods in Ecology and Evolution* 3(2):217–223.
- 550 25. Felsenstein J (1985) Phylogenies and the comparative method. *The American*
551 *Naturalist* 125(1):1–15.
- 552 26. Revell LJ, Chamberlain SA (2014) Rphylip: An r interface for phylip. *Methods in*
553 *Ecology and Evolution* 5(9):976–981.
- 554 27. Adams DC, Collyer M, Kaliontzopoulou A, Sherratt E (2016) Geomorph: Software
555 for geometric morphometric analyses.
- 556 28. Ingram T, Mahler DL (2013) SURFACE: Detecting convergent evolution from
557 comparative data by fitting ornstein-uhlenbeck models with stepwise akaike information
558 criterion. *Methods in ecology and evolution* 4(5):416–425.
- 559 29. Jombart T, Devillard S, Balloux F (2010) Discriminant analysis of principal compo-
560 nents: A new method for the analysis of genetically structured populations. *BMC genetics*
561 11(1):94.
- 562 30. Siebert S, Pugh PR, Haddock SH, Dunn CW (2013) Re-evaluation of characters in
563 apolemiidae (siphonophora), with description of two new species from monterey bay, california.
564 *Zootaxa* 3702(3):201–232.
- 565 31. Skaer R (1988) *The formation of cnidocyte patterns in siphonophores* (Academic
566 Press New York).

- 567 32. Skaer R (1991) Remodelling during the development of nematocysts in a siphonophore.
- 568 *Hydrobiologia* (Springer), pp 685–689.
- 569 33. Blyth CR (1972) On simpson's paradox and the sure-thing principle. *Journal of the*
- 570 *American Statistical Association* 67(338):364–366.
- 571 34. Uyeda JC, Zenil-Ferguson R, Pennell MW (2018) Rethinking phylogenetic comparative
- 572 methods. *Systematic Biology* 67(6):1091–1109.
- 573 35. Wagner GP (1996) Homologues, natural kinds and the evolution of modularity.
- 574 *American Zoologist* 36(1):36–43.
- 575 36. Simpson GG (1955) *Major features of evolution* (Columbia University Press: New
- 576 York).
- 577 37. Bode H (1988) Control of nematocyte differentiation in hydra. *The Biology of*
- 578 *Nematocysts* (Elsevier), pp 209–232.
- 579 38. David CN, et al. (2008) Evolution of complex structures: Minicollagens shape the
- 580 cnidarian nematocyst. *Trends in genetics* 24(9):431–438.
- 581 39. Carré D (1972) Study on development of cnidocysts in gastrozooids of muggiaeae kochi
- 582 (will, 1844) (siphonophora, calycophora). *Comptes Rendus Hebdomadaires des Seances de*
- 583 *l'Academie des Sciences Serie D* 275(12):1263.
- 584 40. Purcell JE (1984) The functions of nematocysts in prey capture by epipelagic
- 585 siphonophores (coelenterata, hydrozoa). *The Biological Bulletin* 166(2):310–327.
- 586 41. Thomason J (1988) The allometry of nematocysts. *The Biology of Nematocysts*
- 587 (Elsevier), pp 575–588.
- 588 42. Carré D, Carré C (1980) On triggering and control of cnidocyst discharge. *Marine &*
- 589 *Freshwater Behaviour & Phy* 7(1):109–117.
- 590 43. Hessinger DA (1988) Nematocyst venoms and toxins. *The Biology of Nematocysts*
- 591 (Elsevier), pp 333–368.
- 592 44. Mitra A (2009) Are closure terms appropriate or necessary descriptors of zooplankton
- 593 loss in nutrient–phytoplankton–zooplankton type models? *Ecological Modelling* 220(5):611–

594 620.